

The crystal structure of meurigite

ANTHONY R. KAMPE,^{1,*} JOSEPH J. PLUTH,² AND YU-SHENG CHEN³

¹Mineral Sciences Department, Natural History Museum of Los Angeles County, 900 Exposition Blvd., Los Angeles, California 90007, U.S.A.

²Department of Geophysical Sciences, Center for Advanced Radiation Sources and Materials Research Science and Engineering Center, University of Chicago, 5734 S. Ellis Avenue, Chicago, Illinois 60637-1434, U.S.A.

³Center for Advanced Radiation Sources, University of Chicago, 5640 S. Ellis Avenue, Chicago, Illinois 60637-1434, U.S.A.

ABSTRACT

The crystal structure of meurigite, ideally $[\text{K}(\text{H}_2\text{O})_{2.5}][\text{Fe}_8^{3+}(\text{PO}_4)_6(\text{OH})_7(\text{H}_2\text{O})_4]$, monoclinic, $C2/c$, $a = 29.018(5)$, $b = 5.1892(6)$, $c = 19.695(3)$ Å, $\beta = 106.987(1)^\circ$, $Z = 4$, from the Santa Rita mine, New Mexico, has been solved and refined to $R_1 = 4.69\%$, $wR_2 = 12.6\%$ using 3325 unique [$F_o > 4\sigma(F_o)$] reflections collected using a Bruker 6000 SMART CCD diffractometer and synchrotron radiation of wavelength 0.41328 Å. The structure of meurigite is a framework consisting of face-sharing octahedral $\text{Fe}_2^{3+}\text{O}_6$ dimers, which are linked by sharing corners with corner-sharing dimers and isolated Fe^{3+}O_6 octahedra to form thick slabs of octahedra parallel to the **a-c** plane. PO_4 tetrahedra further link octahedra within the slabs and also link slabs to one another perpendicular to the **a-c** plane. Relatively large channels through the framework along the **b** axis contain disordered K atoms and H_2O molecules, which take part in two overlapping arrays. Partial vacancies in the Fe and P sites may account for discrepancies between the empirical and ideal chemical formulas. Packing considerations suggest that the empirical formula should be based on the total number of large ions ($\text{K} + \text{Na} + \text{O} = 38.5$ per formula unit), which for the chemical analysis provided in the original description yields $[(\text{K}_{0.91}\text{Na}_{0.03})_{20.94}(\text{H}_2\text{O})_{2.56}]_{23.50}[(\text{Fe}_{3.52}\text{Al}_{0.17}\text{Cu}_{0.03})_{27.72}(\text{PO}_4)_{5.48}(\text{CO}_3)_{0.21}(\text{OH})_{7.20}(\text{H}_2\text{O})_{5.23}]$. The meurigite structure is related to those of other fibrous ferric phosphates with 5 Å fiber axes and shows a particularly close relationship with the structure of dufrénite. Crystal chemical evidence suggests that, even if meurigite and phosphofibrite are isostructural, phosphofibrite may qualify as a distinct species based upon its low K content (<0.5 apfu based on a recalculation of the original chemical analysis).

Keywords: Meurigite, phosphofibrite, crystal structure, crystal chemistry, fibrous iron phosphates

INTRODUCTION

Meurigite was first described by Birch et al. (1996) from the Santa Rita mine, Grant Co., New Mexico, where it occurs as tabular, elongated crystals forming spherical and hemispherical clusters to 2 mm across. The authors noted that the fibrous nature of meurigite made single crystal X-ray diffraction study and crystal structure determination impossible. From TEM studies and indexed X-ray powder diffraction patterns, Birch et al. (1996) derived probable space groups $C2$, Cm , and $C2/m$, and unit-cell parameters $a = 29.52(4)$, $b = 5.249(6)$, $c = 18.26(1)$ Å, $\beta = 109.27(7)^\circ$. Meurigite and its Na analog have been noted at several other localities (Birch et al. 1996; Walenta and Theye 2001; Kolitsch 1999; Kolitsch pers. comm.); however, crystals at these localities have generally been smaller and even less suitable for single-crystal X-ray diffraction work.

Birch et al. (1996) noted meurigite to be a member of the group of fibrous ferric phosphates with a discrete 5 Å fiber axis (which corresponds to the sum of the edges of one octahedron and one tetrahedron). They pointed out that compositionally

meurigite is most closely related to kidwellite and phosphofibrite; however, the structural relationships between these minerals were at that time unclear, because none of their structures were known. Kolitsch (2004) determined the structure of kidwellite, as well as that of the “laubmannite” of Moore (1970).

Kolitsch (1999) using transmission electron microscopy and X-ray powder diffraction concluded that meurigite and phosphofibrite were the same mineral species; however, phosphofibrite type material was not examined in this study. A proposal to discredit one of these species has never been submitted to the Commission on New Minerals and Mineral names.

Continuing efforts to unravel the structural relationships and crystal chemistry among the fibrous ferric iron phosphates led to the present study in which synchrotron radiation has been successfully employed to collect single-crystal X-ray diffraction data from a small crystal fragment of meurigite from the type specimen and to finally determine the structure of this mineral.

STRUCTURE DETERMINATION

For structure data collection a $100 \times 40 \times 5$ μm crystal fragment of meurigite from the type specimen was mounted on the tip of a glass fiber. Data were collected at GSECARS and

* E-mail: akampf@nhm.org

ChemMatCARS (CARS = Consortium for Advanced Radiation Sources) sectors 13 and 15 at the Advanced Photon Source, Argonne, Illinois. The data set used in the refinement was collected using radiation from a water-cooled diamond (111) crystal at a wavelength of 0.41328 Å with higher harmonics removed using vertical Pt-coated Si mirrors and apertures to produce a $200 \times 200 \mu\text{m}^2$ beam. Data were recorded using a Bruker 6000 SMART CCD (charge-coupled device) detector at fixed angle $5^\circ 2\theta$ and scanning ϕ in 0.5° steps with 1 second counting per frame. The CCD detector was mounted on a Huber 4-circle diffractometer with the ω axis of the diffractometer in the plane of the ring. A full rotation of the ϕ axis yielded 721 frames with $\chi = 0^\circ$. Reflections were sharp with no evidence of streaking or doubling. Unit-cell parameters were refined by least squares using 6950 reflections and are given in Table 1. Data were integrated and corrected for Lorentz, polarization, and background effects using Bruker software (SAINTPLUS). Systematic errors, such as beam decay and absorption, were corrected with the program SADABS on the basis of the intensities of equivalent reflections. The crystal structure was solved and refined using SHELXTL (Sheldrick 1997).

The location of Fe and P atoms and all octahedral and tetrahedral O atoms was straightforward and revealed an octahedral-tetrahedral framework with channels along the **b** axis. Four peaks with significant electron density within the channels were assigned as two K (K1 and K2) and two O (OW3 and OW4) sites based upon distances to framework O atoms and to one other. The channel sites are clearly too close together to be fully occupied and their refined occupancies bear this out. All non-hydrogen atoms were located and refined with anisotropic displacement parameters to an R_1 value of 4.87%. Because of the large anisotropic displacement parameters for OW3 and OW4, an effort was made to split each of these sites; however,

the results were clearly inferior to those obtained with unsplit sites. No hydrogen positions were located from the structure determination, but OH and H₂O groups were assigned using bond valence calculations.

Because the chemical analysis of the type material by Birch et al. (1996) suggested the possibility of deficiencies in Fe and P, as well as minor substitution of Al for Fe and CO₃ for PO₄, an attempt was made to refine the occupancies of these sites. The resulting site occupancies, Fe1 0.94, Fe2 0.94, Fe3 0.92, Fe4 0.93, P1 0.93, P2 0.87, P3 0.93, and improved R_1 value of 4.69% suggest that site deficiencies may, in fact, exist; however, the bond-valence totals are consistent with full occupancies for all except the P2 site. An attempt to refine the Fe sites as mixtures of Fe and Al yielded Al contents that were unreasonably high and did not improve the R_1 value. The final reported results include the refined occupancies for the Fe and P sites. The largest residual peak was $1.9 \text{ e}\text{\AA}^{-3}$ located at 0.204, 0.850, 0.219 and deepest hole was $-1.2 \text{ e}\text{\AA}^{-3}$ located at 0.109, 0.601, 0.154.

Table 1 gives the details of the data collection and structure refinement, Table 2 the final fractional coordinates and displacement parameters, Table 3 interatomic distances, and Table 4 the bond valences.

The unit-cell parameters refined from the structure data differ significantly from those provided by Birch et al. (1996) based upon refined powder data: $a = 29.52(4)$, $b = 5.249(6)$, $c = 18.26(1)$ Å, $\beta = 109.27(7)^\circ$; however, when the powder data of Birch et al. (1996) are reindexed based upon the powder data calculated from the structure, they yield cell parameters in close agreement with ours: $a = 29.02(2)$, $b = 5.176(3)$, $c = 19.67(1)$ Å, $\beta = 107.17(6)^\circ$.

DESCRIPTION OF THE STRUCTURE

The structure of meurigite is a framework of Fe³⁺O₆ octahedra and PO₄ tetrahedra with channels along the **b** (5 Å) axis containing K atoms and H₂O molecules (Fig. 1). The most unusual feature of the structure is an octahedral face-sharing dimer. The dimers are linked by sharing corners with corner-sharing dimers and isolated octahedra forming thick slabs of octahedra parallel to the **a-c** plane. Tetrahedra further link octahedra within the slabs and also link slabs to one another perpendicular to the **a-c** plane.

TABLE 1. Data collection and structure determination details for meurigite

Ideal formula	[K(H ₂ O) _{2.5}][Fe ₃ ³⁺ (PO ₄) ₆ (OH) ₇ (H ₂ O) ₄]
Crystal system	monoclinic
Space group	C2/c
<i>a</i>	29.018(5) Å
<i>b</i>	5.1892(6) Å
<i>c</i>	19.695(3) Å
β	106.987(5)°
<i>V</i>	2836.3(7) Å ³
<i>Z</i>	4
Crystal size	100 × 40 × 5 μm
Temperature	273(2) K
Wavelength	0.41328 Å
Absorption coefficient	2.248 mm ⁻¹
<i>F</i> (000)	2491
Theta range for data collection	1.71–16.84°
Index ranges	−36 ≤ <i>h</i> ≤ 40, −7 ≤ <i>k</i> ≤ 6, −27 ≤ <i>l</i> ≤ 25
Reflections collected	14144
Independent reflections	3922 [<i>R</i> (int) = 0.0343]
Reflections, $F_o > 4\sigma(F_o)$	3325
Completeness to theta = 16.33°	95.9%
Absorption correction	None
Refinement method	Full-matrix least-squares on <i>F</i> ²
Data/restraints/parameters	3922/0/266
Goodness-of-fit on <i>F</i> ²	1.233
Final <i>R</i> indices [$F_o > 4\sigma(F_o)$]	<i>R</i> ₁ = 0.0469, <i>wR</i> ₂ = 0.1261
<i>R</i> indices (all data)	<i>R</i> ₁ = 0.0581, <i>wR</i> ₂ = 0.1372
Largest diff. peak and hole	1.9 and −1.2 eÅ ⁻³

Notes: $R_{\text{int}} = \sum |F_o^2 - F_o^2(\text{mean})| / \sum F_o^2$. $\text{GoF} = S = \{\sum [w(F_o^2 - F_c^2)] / (n - p)\}^{1/2}$. $R_1 = \sum ||F_o| - |F_c|| / \sum |F_o|$. $wR_2 = \{\sum [w(F_o^2 - F_c^2)]^2 / \sum [w(F_o^2)]^2\}^{1/2}$; $w = 1 / [\sigma^2(F_o^2) + (aP)^2 + bP]$, where a is 0, b is 12.994, and P is $[2F_c^2 + \text{Max}(F_o, 0)] / 3$.

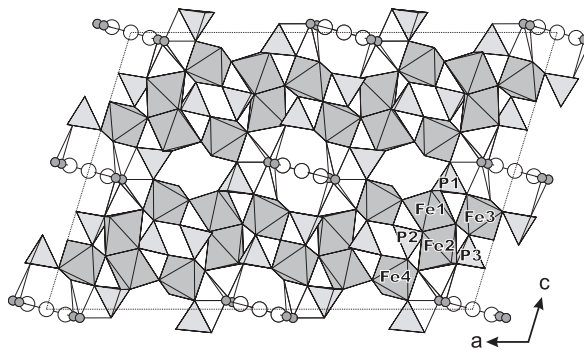


FIGURE 1. Structure of meurigite viewed down the **b** axis. Iron and P polyhedra are labeled. Small shaded circles are partially occupied K1 and K2 sites. Large open circles are partially occupied OW3 and OW4 sites.

TABLE 2. Atom coordinates, occupancies and displacement parameters (\AA^2) for meurigite

Atom	x	y	z	occ.	U_{11}	U_{22}	U_{33}	U_{23}	U_{13}	U_{12}	U_{eq}
K1	0.4309(5)	0.548(3)	0.4743(5)	0.264(11)	0.087(9)	0.150(15)	0.041(5)	0.009(6)	0.001(5)	0.052(9)	0.096(7)
K2	0.4150(5)	0.308(3)	0.4687(5)	0.198(10)	0.076(8)	0.069(9)	0.031(5)	0.011(4)	0.005(4)	-0.032(6)	0.061(5)
Fe1	0.3257(1)	0.4157(1)	0.6374(1)	0.937(5)	0.0070(3)	0.0040(3)	0.0077(3)	-0.0001(2)	0.0019(2)	0.0006(2)	0.0063(2)
Fe2	0.3785(1)	0.3837(1)	0.7894(1)	0.938(5)	0.0070(3)	0.0043(3)	0.0082(3)	0.0003(2)	0.0022(2)	-0.0003(2)	0.0065(2)
Fe3	0.4504(1)	0.1396(1)	0.6688(1)	0.922(5)	0.0055(3)	0.0044(3)	0.0071(3)	0.0000(2)	0.0014(2)	0.0001(2)	0.0058(2)
Fe4	0.2952(1)	0.1875(1)	0.8794(1)	0.929(5)	0.0068(3)	0.0055(4)	0.0088(3)	0.0005(2)	0.0024(2)	-0.0008(2)	0.0070(2)
P1	0.3514(1)	0.9314(2)	0.5494(1)	0.927(8)	0.0051(6)	0.0037(6)	0.0064(6)	-0.0011(4)	0.0015(4)	-0.0004(4)	0.0051(4)
P2	0.3053(1)	0.9043(2)	0.7390(1)	0.866(8)	0.0045(6)	0.0009(6)	0.0069(6)	-0.0006(4)	0.0024(4)	-0.0001(4)	0.0040(4)
P3	0.4459(1)	0.8815(2)	0.8119(1)	0.934(8)	0.0059(6)	0.0038(6)	0.0076(6)	0.0009(4)	0.0019(4)	-0.0008(4)	0.0058(4)
O1	0.4041(1)	0.9978(7)	0.5846(2)		0.008(2)	0.017(2)	0.016(2)	-0.003(1)	0.001(1)	-0.002(1)	0.0141(7)
O2	0.3418(1)	0.9391(7)	0.4688(2)		0.013(2)	0.014(2)	0.011(2)	-0.001(1)	0.003(1)	-0.002(1)	0.0127(7)
O3	0.3182(1)	0.1243(7)	0.5720(2)		0.016(2)	0.013(2)	0.017(2)	-0.006(1)	0.005(1)	0.001(1)	0.0152(7)
O4	0.3398(1)	0.6584(7)	0.5710(2)		0.021(2)	0.009(2)	0.017(2)	0.004(1)	0.006(1)	-0.002(1)	0.0156(7)
O5	0.2529(1)	0.8770(7)	0.6957(2)		0.009(2)	0.014(2)	0.019(2)	-0.007(1)	-0.001(1)	0.001(1)	0.0154(7)
O6	0.3117(1)	0.9129(7)	0.8204(2)		0.021(2)	0.007(2)	0.018(2)	0.000(1)	0.009(1)	-0.001(1)	0.0146(7)
O7	0.3269(1)	0.1619(6)	0.7199(2)		0.015(2)	0.008(2)	0.012(2)	0.001(1)	0.004(1)	-0.001(1)	0.0118(7)
O8	0.3347(1)	0.6691(6)	0.7237(2)		0.012(2)	0.009(2)	0.011(2)	0.001(1)	0.004(1)	0.001(1)	0.0105(6)
O9	0.4167(1)	0.0966(7)	0.8328(2)		0.021(2)	0.011(2)	0.017(2)	0.004(1)	0.007(1)	0.008(1)	0.0161(7)
O10	0.4299(1)	0.6221(7)	0.8344(2)		0.018(2)	0.008(2)	0.015(2)	0.003(1)	0.004(1)	-0.005(1)	0.0139(7)
O11	0.4379(1)	0.8738(7)	0.7312(2)		0.012(2)	0.012(2)	0.012(2)	0.001(1)	0.004(1)	-0.003(1)	0.0134(7)
O12	0.5004(1)	0.9152(7)	0.6473(2)		0.009(2)	0.019(2)	0.017(2)	-0.004(1)	0.002(1)	0.001(1)	0.0154(7)
OH1	0.2564(1)	0.4681(7)	0.6052(2)		0.009(2)	0.012(2)	0.023(2)	-0.005(1)	0.004(1)	0.001(1)	0.0146(7)
OH2	0.3991(1)	0.3834(6)	0.6920(2)		0.011(2)	0.008(2)	0.013(2)	0.001(1)	0.002(1)	0.001(1)	0.0110(6)
OH3	0.3444(1)	0.4240(6)	0.8609(2)		0.013(2)	0.007(2)	0.014(2)	0.000(1)	0.007(1)	-0.002(1)	0.0110(6)
OH4	0.5	0.3041(9)	0.75		0.012(2)	0.012(2)	0.012(2)	0	0.000(2)	0	0.0127(9)
OW1	0.2770(1)	0.4744(7)	0.9450(2)		0.015(2)	0.016(2)	0.016(2)	-0.001(1)	0.004(1)	0.005(1)	0.0155(7)
OW2	0.4636(2)	0.4287(8)	0.6062(2)		0.037(2)	0.016(2)	0.019(2)	0.003(1)	0.004(2)	-0.013(2)	0.0251(9)
OW3	0.4515(4)	0.9870(40)	0.4807(4)	0.903(33)	0.061(7)	0.432(31)	0.014(3)	-0.030(7)	0.021(4)	-0.092(11)	0.167(11)
OW4	0.5	0	0.5	0.629(24)	0.183(38)	0.120(20)	0.025(8)	0.020(9)	0.045(13)	0.000(18)	0.106(15)

For OW3 and OW4 refined with isotropic displacement parameters:
 OW3 0.4512(4) 0.0168(2) 0.4809(6) 0.623(33) 0.051(4)
 OW4 0.5 0 0.5 0.518(21) 0.067(8)

TABLE 3. Selected bond distances (\AA) in meurigite

K1-OW2	2.567(10)	Fe1-OH1	1.940(3)	Fe3-O1	1.948(3)	P1-O1	1.524(3)	H-bond donor-receptor	
K1-OH3	2.835(11)	Fe1-O4	1.943(4)	Fe3-O11	1.950(3)	P1-O2	1.531(3)	OH2-O11	2.890(5)
K1-O10	2.887(11)	Fe1-O3	1.956(3)	Fe3-O12	2.000(4)	P1-O3	1.542(4)	OH3-O6	2.743(5)
K1-OW3	2.968(27)	Fe1-O7	2.084(3)	Fe3-OH4	2.003(2)	P1-O4	1.544(4)	OW1-O3	2.793(5)
K1-OW4	3.030(18)	Fe1-OH2	2.096(3)	Fe3-OW2	2.049(4)	<P1-O>	1.535	OW1-O4	2.704(5)
K1-O2	3.261(12)	Fe1-O8	2.105(3)	Fe3-OH2	2.102(3)			OW2-O12	2.768(5)
K1-O9	3.266(13)	<Fe1-O>	2.037	<Fe3-O>	2.021	P2-O5	1.515(3)	OW3-O9	2.825(13)
K1-O1	3.426(13)					P2-O6	1.560(4)	OW3-OW3	2.698(40)
<K1-O>	3.03					P2-O7	1.569(4)	OW4-O12	2.930(4)
						P2-O8	1.569(4)		
K2-OW2	2.735(11)	Fe2-O9	1.903(3)	Fe4-O5	1.974(3)	<P2-O>	1.553		
K2-O10	2.826(11)	Fe2-O10	1.940(3)	Fe4-OH1	1.975(3)				
K2-OH3	2.847(13)	Fe2-OH3	1.955(3)	Fe4-O6	1.984(3)	P3-O9	1.528(4)		
K2-OW4	2.852(15)	Fe2-O7	2.062(3)	Fe4-O2	1.991(3)	P3-O10	1.530(3)		
K2-O2	2.859(11)	Fe2-O8	2.126(3)	Fe4-OH3	1.994(3)	P3-O11	1.538(4)		
K2-O1	2.884(10)	Fe2-OH2	2.171(3)	Fe4-OW1	2.136(4)	P3-O12	1.542(4)		
K2-O9	3.414(14)	<Fe2-O>	2.051	<Fe4-O>	2.015	<P3-O>	1.535		
<K2-O>	2.95								

TABLE 4. Bond-valence summations for meurigite

	O1	O2	O3	O4	O5	O6	O7	O8	O9	O10	O11	O12	OH1	OH2	OH3	OH4	OW1	OW2	OW3	OW4	Σ
K1	0.01	0.01							0.01	0.03					0.04			0.08	0.03	0.02 x2↓	0.23
K2	0.03	0.03							0.01	0.03					0.03			0.04		0.03 x2↓	0.20
Fe1			0.59	0.61			0.42	0.39					0.61	0.40							3.02
Fe2							0.44	0.37	0.68	0.61				0.33	0.59						3.02
Fe3	0.60									0.60	0.52			0.40		0.52 x2↓		0.46			3.10
Fe4		0.53			0.56	0.54							0.56		0.53		0.36				3.08
P1	1.29	1.26	1.23	1.22																	5.00
P2					1.32	1.17	1.14	1.14													4.77
P3									1.27	1.27	1.24	1.23									5.01
Σ	1.93	1.83	1.82	1.83	1.88	1.71	2.00	1.90	1.97	1.94	1.84	1.75	1.17	1.13	1.19	1.04	0.36	0.58	0.03	0.10	

Notes: K-O, Fe-O, and P-O bond strengths from Brese and O'Keeffe (1991). K1 and K2 bond strengths have been adjusted to reflect their respective site occupancies. Despite the less than full occupancies indicated for the Fe and P sites, these sites are assumed to be fully occupied for the bond-valence calculations. Valence summations are expressed in valence units.

There are two types of channels in the framework. The larger, centered at $x = 0$ and $z = 0$, is elliptical in cross-section with K sites situated toward either side and H_2O sites (OW3 and OW4) toward the center. The smaller channel, centered at $x = \frac{1}{4}$ and $z =$

0, is empty, except for likely H atoms associated with OH1 and OW1. The K1, K2, OW3, and OW4 sites in the large channels lie approximately in a plane perpendicular to the c axis (Fig. 2a).

There are several key factors that must be considered in un-

understanding the interrelationships between K1, K2, OW3, and OW4 in the large channels. (1) Adjacent K1 and K2 sites cannot be simultaneously occupied; nor can adjacent OW3 and OW4 sites. [Note that the latter requirement is in contradiction to the nearly full refined occupancy (0.90) for the OW3 site; however, using isotropic displacement parameters for the OW3 and OW4 sites, their occupancies refine to 0.62 and 0.52, respectively.] (2) The OW3 site is located 2.97 and 2.35 Å from the closest K1 sites and 1.95 Å from the K2 site, the latter two distances being unreasonably short for K-O bonds; clearly the OW3 site adjacent to an occupied K2 site must be vacant, as must the OW3 site 2.35 Å away from an occupied K1 site. (3) The OW4 site is 3.03 Å from K1 and 2.85 Å from K2, so that a H₂O at this site could bond to both K1 and K2. (4) Considering the low occupancies for the K1 and K2 sites indicated by the structure refinement (0.264 and 0.198, respectively), it seems possible that locally H₂O molecules at OW3 or OW4 have no nearby K with which to bond.

Based upon bond-length considerations, the K1, K2, OW3, and OW4 sites shown in Figure 2a appear to represent two equivalent networks of atoms that are offset along the **b** axis (the channel direction) by one cell length with respect to one another. One such network is shown in Figure 2b. If one of these networks of K and OW sites were fully occupied, there would be no space for any additional large ions in the channels. This apparently does not tell the whole story since in that event the K content would be more than twice that provided by the occupancies for the K1 and K2 sites indicated by the structure refinement (1.00 vs. 0.46), as well as that provided by the chemical analysis. One way around this would be to assume that H₂O molecules take the place (though not necessarily the exact positions) of approximately half of the K atoms in the channel network, with hydrogen bonds linking the H₂O molecules to

one another. Assuming that this is the case, the channel would contribute approximately one K and 2½ H₂O per formula unit (4 K and 10 H₂O per unit cell). This appears to be a maximum content for the channel, though lower K content would allow higher H₂O content and vice versa.

As noted above, hydrogen atom positions could not be determined from the structure analysis. It was impossible to devise a completely unambiguous hydrogen bonding scheme based upon bond valence calculations, O-O distances and geometrical factors. One possible scheme is indicated by the O_{donor}-O_{acceptor} distances listed in Table 3. There appear to be no likely H-bond acceptors associated with OH1 and OH4 or with one of the H atoms of OW2.

The formula of meurigite

The ideal formula for meurigite suggested by the structure analysis, assuming full occupancies for all atoms in the framework and taking into consideration the discussion of the channel contents above, is $KFe_8^{3+}(PO_4)_6(OH)_7 \cdot 6.5H_2O$ or, separating the formula into framework and channel components, $[K(H_2O)_{2.5}][Fe_8^{3+}(PO_4)_6(OH)_7(H_2O)_4]$ ($Z = 4$). The ideal formula perhaps would be better stated in all whole numbers as $[K_2(H_2O)_5][Fe_{16}^{3+}(PO_4)_{12}(OH)_{14}(H_2O)_8]$ ($Z = 2$); however, for comparison with the formula proposed by Birch et al. (1996), we prefer the former. The chemical composition based on this ideal formula is K₂O 3.65, Fe₂O₃ 49.45, P₂O₅ 32.96, H₂O 13.95 wt% and the calculated density is 3.025 g/cm³.

Birch et al. (1996) provided three possible ideal formulas and chose $KFe_7^{3+}(PO_4)_5(OH)_7 \cdot 8H_2O$ because it gave the best fit between the calculated density (2.89 g/cm³) and the measured density (2.96 g/cm³). Their chemical analysis is provided in Table 5 and from this they derived the empirical formula $(K_{0.85}Na_{0.03})_{\Sigma 0.88}(Fe_{7.01}^{3+}Al_{0.16}Cu_{0.02})_{\Sigma 7.19}(PO_4)_{5.11}(CO_3)_{0.20}(OH)_{6.7} \cdot 7.25H_2O$

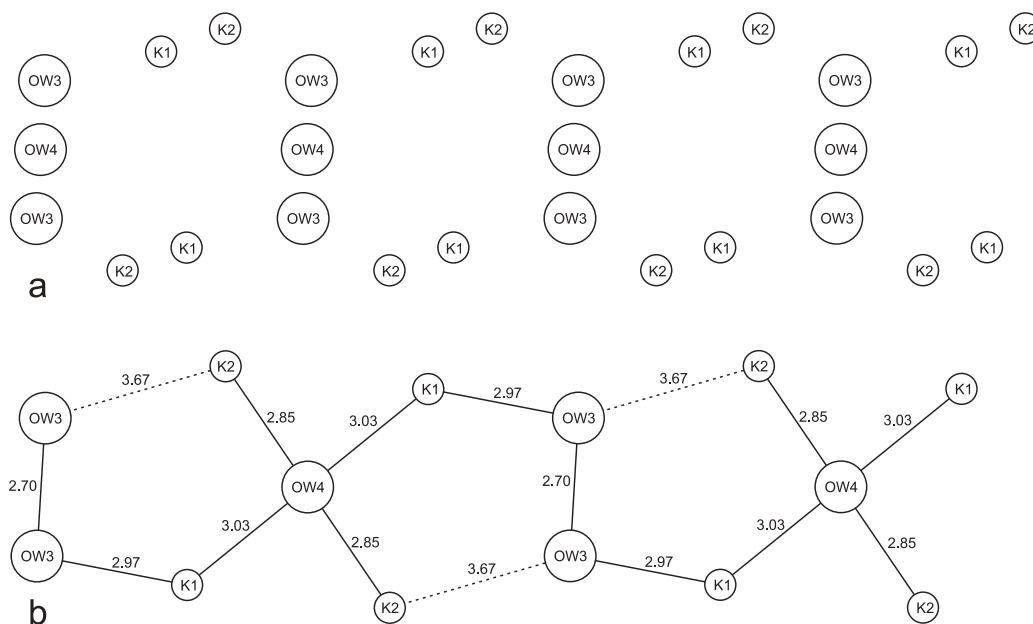


FIGURE 2. (a) Channel sites in meurigite structure viewed down the *c* axis with the channel direction (**b** axis) horizontal. (b) One network of K1, K2, OW3, and OW4 sites with distances in Å shown.

(based on 35 O atoms).

Packing considerations suggest that a better basis for calculating the formula may be the total number of large ions indicated by the structure. The framework contains 35 O atoms and the channel contains 3.5 K + Na + O, for a total of 38.5 K + Na + O per formula unit. This yields the empirical formula $[(K_{0.91}Na_{0.03})_{\Sigma 0.94}(H_2O)_{2.56}]_{\Sigma 3.50}[(Fe_{7.52}^{3+}Al_{0.17}Cu_{0.03})_{\Sigma 7.72}(PO_4)_{5.48}(CO_3)_{0.21}(OH)_{7.20}(H_2O)_{5.23}]$ and a calculated density of 2.95 g/cm³. The validity of this approach is supported by the close match between the calculated and measured densities, as well as by the less than full refined Fe and P occupancies in the structure analysis. The refined occupancies for the Fe and P sites yield totals per formula unit of 7.45 Fe and 5.45 P; however, because the Fe total does not take into consideration that the Fe site occupancy values are lowered somewhat by the likely presence of a small amount of Al in the sites, the total occupancy of the octahedral sites is expected to be higher than 7.45.

It seems most likely that the CO₃²⁻ in the structure partially replaces PO₄, as it does in some other phosphates, notably carbonate-bearing apatites. The C atom may be positioned at the center of one or more of the four faces of a PO₄ tetrahedron as observed in holtehdahlite (Rømming and Raade 1989). The very low refined occupancy for the P2 site noted above indicates that most of the CO₃ in the structure probably occurs in the vicinity of this site. The small amount of C present in meurigite and the weak scattering of C atoms would make them undetectable in the difference map. An FTIR spectrum obtained for type meurigite did exhibit a small peak in the 1400–1500 cm⁻¹ region, consistent with the presence of a small amount of CO₃.

It should be noted that the empirical formula provided above gives a somewhat distorted “picture” of the likely distribution of O, OH, and H₂O in the structure. It is very likely that all framework O sites are fully occupied. (A refinement of the occupancies of the framework O sites indicated very little deviation from full occupancies.) The local charge balance within the structure would be maintained by distributing the “surplus” H atoms among the framework O atoms leading, among other things, to the PO₄ groups taking on some PO₃(OH) character. This could also serve to ameliorate the low bond valence sums for O6 (1.71) and O12 (1.75), in Table 4. In addition, it is conceivable

that some channel H₂O could be H₃O⁺.

There are relatively few published chemical analyses of meurigite. The chemical analysis of a K-poor meurigite (see Table 5) from the Kněžská hora quarry, Bohemia, Czech Republic reported by Sejkora et al. (2000) yields the empirical formula $[K_{0.62}(H_2O)_{1.26}(CO_3)_{0.54}][Fe_{7.20}^{3+}Al_{0.54}]_{\Sigma 7.74}(PO_4)_{5.66}(CO_3)_{0.34}(OH)_{5.10}(H_2O)_{6.26}]$ based upon K + O = 38.5. Note that because the total of P and C exceeds the theoretical framework limit, we have assumed the excess CO₃ to be accommodated in the channel.

Walenta and Theye (2001) reported an analysis (see Table 5) of meurigite from the Clara mine, Black Forest, Germany (with H₂O by difference) that yields $[K_{0.74}(H_2O)_{2.76}]_{\Sigma 3.50}[Fe_{7.66}^{3+}Cu_{0.04}]_{\Sigma 7.70}(PO_4)_{5.47}(OH)_{7.39}(H_2O)_{5.72}]$ based upon K + O = 38.5. Interestingly, this formula suggests Fe and P site vacancies that are very similar to those indicated for type meurigite.

The relationship between meurigite and phosphofibrite

Walenta and Dunn (1984) described the new species phosphofibrite, also from the Clara mine. If phosphofibrite is equivalent to meurigite, it should be possible to present its empirical formula based on K + O = 38.5; however, the empirical formula calculated using the analysis of Walenta and Dunn (see Table 5) on this basis has impossibly high totals for the framework cations: $[K_{0.53}(H_2O)_{2.97}]_{\Sigma 3.50}[(Fe_{7.61}^{3+}Al_{0.38}Cu_{0.43})_{\Sigma 8.42}(PO_4)_{6.24}(OH)_{6.62}(H_2O)_{3.41}]$. The likely source of the inconsistency is the H₂O content calculated by difference, which is significantly lower than that reported for meurigite. An empirical formula that fits the meurigite format can be derived, if it is assumed that the H₂O by difference is in error, by basing the formula on octahedral cations = 8, with K + O = 38.5 and sufficient H for charge balance. This yields $[K_{0.50}(H_2O)_{3.00}]_{\Sigma 3.50}[(Fe_{7.23}^{3+}Cu_{0.41}Al_{0.36})_{\Sigma 8.00}(PO_4)_{5.94}(OH)_{6.29}(H_2O)_{4.97}]$. It should be noted, however, that if there are vacancies in the octahedral sites, as is suggested for the other meurigites analyzed, the empirical formula would have less than 0.50 K.

To further clarify the crystal-chemical relationship between phosphofibrite and meurigite, the polished microprobe mount used in the original description of phosphofibrite was reanalyzed by EPMA. This specimen in the collection of the Smithsonian Institution (no. 150230) apparently represents the only known type specimen of phosphofibrite. The averages and ranges of nine analyses are presented in Table 5.

The sample exhibited marked degassing in the electron beam. To minimize this effect, the analyses were conducted at relatively low voltage and current (15 kV, 15 nA) using a focused beam scanning at 5000×. The narrow fiber diameters required that all scanned areas include grain boundaries, which probably slightly lowered the analytical values, an effect opposite to that generally produced by degassing. Walenta and Dunn (1984) did not report the conditions under which their analysis was conducted; however, degassing during their analysis could account for significantly high analytical values and a low water-by-difference value.

Our analytical totals were significantly lower than that obtained by Walenta and Dunn (1984); however, the relative amounts of the major components compare favorably. Our water-by-difference is much higher than the water contents reported for meurigite and is clearly too high to be accommodated in the meurigite structure. If we assume that our analytical values are

TABLE 5. Chemical analyses of meurigite and phosphofibrite

	1	2	3	4	5	5 ranges
Na ₂ O	0.07	–	–	–	–	
K ₂ O	3.37	2.78	2.33	1.90	1.55	1.38–1.77
CaO	–	–	–	–	0.16	0.13–0.21
CuO	0.16	0.25	–	2.60	2.84	2.31–3.12
Fe ₂ O ₃	47.4	48.7	45.85	46.6	42.7	41.8–43.6
Al ₂ O ₃	0.70	–	2.20	1.50	0.92	0.20–1.54
P ₂ O ₅	30.7	30.9	32.06	34.0	29.7	28.5–30.3
As ₂ O ₃	0.03	–	–	–	0.88	0.77–1.03
CO ₂	0.73	n.d.	3.08	n.d.	n.d.	
H ₂ O*	16.2	[17.37]	14.48	[13.4]	[21.25]	[19.8–22.6]
	99.37	100.00	100.00	100.00	100.00	

Notes: 1 = Meurigite (type), Santa Rita mine, Grant Co., New Mexico (Birch et al. 1996). 2 = Meurigite, Clara mine, Black Forest, Germany (Walenta and Theye 2001). 3 = Meurigite, Kněžská hora quarry, Bohemia, Czech Republic (Sejkora et al. 2000). 4 = Phosphofibrite (type), Clara mine, Black Forest, Germany (Walenta and Dunn 1984). 5 = Phosphofibrite (type), Clara mine, Black Forest, Germany (This study; Cameca SX50 electron microprobe operated at 15 kV and 15 nA; standards: olivine for Fe, Ca₂P₂O₇ for Ca and P, microcline for K, albite for Na and Al, copper metal for Cu, FeAs₂ for As).

* H₂O values in brackets are by difference.

too low (and our water-by-difference too high), an empirical formula consistent with that provided for meurigite can be derived on the same basis as that used above for the analysis of Walenta and Dunn (1984), i.e., based upon 8 octahedral cations with $K + Ca + O = 38.5$ and sufficient H for charge balance. This yields $[K_{0.45}Ca_{0.04}(H_2O)_{3.01}]_{\Sigma 3.50}[(Fe_{7.27}^{3+}Cu_{0.48}Al_{0.25})_{\Sigma 8.00}(PO_4)_{5.69}(AsO_4)_{0.10}(OH)_{6.77}(H_2O)_{5.07}]$. It should be noted that CO_2 was not measured; however, a small amount of CO_3^{2-} could be readily accommodated without changing the formula significantly.

The evidence presented by Kolitsch (1999) strongly suggests that meurigite and phosphofibrite have very similar, if not identical, structures. If their structures are identical, the empirical formula above clearly indicates less than 0.5 K per formula unit (if it is assumed that there was no loss of alkali atoms during the analysis). Whether this would qualify phosphofibrite as the hypothetical H_2O -dominant end-member of a series between $[(H_2O)_{3.5}][Fe_8^{3+}(PO_4)_6(OH)_6(H_2O)_5]$ and $[K(H_2O)_{2.5}][Fe_8^{3+}(PO_4)_6(OH)_7(H_2O)_4]$ is not clear. Assuming an "ideal" framework in which all non-hydrogen sites are fully occupied by Fe^{3+} , P, and O, valence balance (see Table 4) dictates the assignments of O, OH, and H_2O within the framework and, therefore, an H_2O end-member would not be possible; however, a hydronium end-member, $[(H_3O)(H_2O)_{2.5}][Fe_8^{3+}(PO_4)_6(OH)_7(H_2O)_4]$, may theoretically be possible. Evidently, additional chemical analyses of other phosphofibrite and meurigite specimens are necessary to clarify the relationship between these two minerals.

COMPARISONS TO OTHER STRUCTURES

Face-sharing octahedral dimers have been previously reported in the structures of five phosphate minerals: trolleite (Moore and Araki 1974), holtedahlite (Rømming and Raade 1989), raadeite (Chopin et al. 2001), kidwellite (Kolitsch 2004), and "laubmannite" (Kolitsch 2004). The structures of trolleite, holtedahlite, and raadeite are all dense-packed and bear little resemblance to that of meurigite. The structures of kidwellite and "laubmannite" are more open, with channels running along their 5 Å axes, as in meurigite.

The face-sharing octahedral trimer, first referred to as the *h* cluster by Moore (1965), occurs in the structures of several phosphates: lazulite (Lindberg and Christ 1959), scorzalite (Lindberg and Christ 1959), beraunite (Moore and Kampf 1992), rockbridgite (Moore 1970), dufrénite (Moore 1970), burangaite (Selway et al. 1997), barbosalite (Redhammer et al. 2000), and souzalite (Le Bail et al. 2003). In addition, chains of face-sharing octahedra closely resembling the *h* cluster occur in the structure of lipscombite (Vencato et al. 1989; Yakubovich et al. 2006). Of these minerals, beraunite and dufrénite (and isostructural burangaite) have relatively open structures with channels along their 5 Å axes.

The channel structures of dufrénite, beraunite, kidwellite, and "laubmannite" viewed down their 5 Å axes (Fig. 3) can be compared with that of meurigite (Fig. 1). While all five structures are distinct in their arrangements of octahedra and tetrahedra, they all share similar motifs locally. Furthermore, the similar

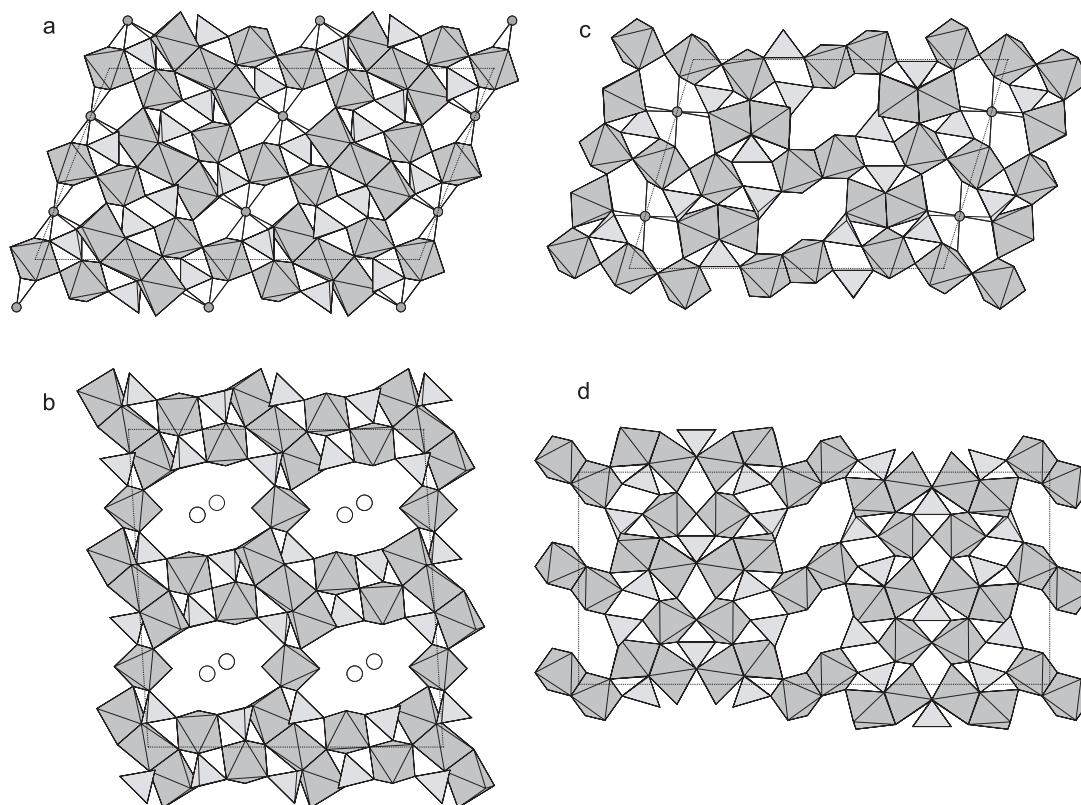


FIGURE 3. Structures of (a) dufrénite, (b) beraunite, (c) kidwellite, and (d) "laubmannite" viewed down the 5 Å axis.

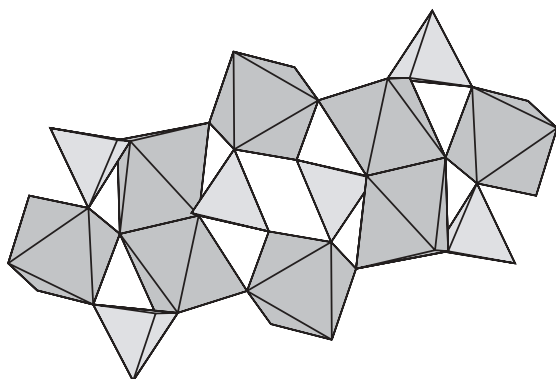


FIGURE 4. Grouping of octahedra and tetrahedra in the structures of meurigite and dufrénite viewed down the **b** (5 Å) axis.

motifs seen in two dimensions in Figure 3 generally are comparable in the third dimension, extending along the 5 Å axes, as well. The structure that bears the greatest similarity to meurigite in this respect is that of dufrénite. These structures have the identical groupings of octahedra and tetrahedra shown in Figure 4. In meurigite, all octahedra and tetrahedra are part of these groupings, which link to one another by sharing octahedral and tetrahedral corners. In dufrénite, one octahedron (corresponding to the Fe at 0,0,0) is not part of this grouping and the groupings themselves actually overlap, with some octahedra and tetrahedra being shared by adjacent groupings.

ACKNOWLEDGMENTS

This structure data collection was performed at GeoSoilEnviroCARS (GSECARS), Sector 13, and ChemMatCARS, Sector 15, Advanced Photon Source at Argonne National Laboratory. GSECARS and ChemMatCARS are supported by the National Science Foundation, Department of Energy, and W.M. Keck Foundation. Use of the Advanced Photon Source was supported by the U.S. Department of Energy, Basic Energy Sciences, Office of Energy Research, under contract no. W-31-109-ENG-38. J.J.P. thanks the Materials Research Science and Engineering Center at The University of Chicago for support. This study was also funded in part by the John Jago Trelawney Endowment to the Mineral Sciences Department of the Natural History Museum of Los Angeles County. We thank William D. Birch of the Museum of Victoria (Melbourne, Australia) for providing the sample of meurigite used in this study, Pete J. Dunn of the United States National Museum of Natural History (Smithsonian Institution) for providing the type specimen of phosphofibrite, Ian M. Steele of the University of Chicago for conducting the EMP analyses of type phosphofibrite, Paul M. Adams of the Aerospace Corporation (Los Angeles) for running the FTIR spectrum of meurigite, and Uwe Kolitsch of the University of Vienna (Austria) for providing information on his research on meurigite and phosphofibrite and for providing comments on the manuscript.

REFERENCES CITED

- Birch, W.D., Pring, A., Self, P.G., Gibbs, R.B., Keck, E., Jensen, M.C., and Foord, E.E. (1996) Meurigite, a new fibrous iron phosphate resembling kidwellite. *Mineralogical Magazine* 60, 787–793.
- Brese, N.E. and O’Keeffe, M. (1991) Bond-valence parameters for solids. *Acta Crystallographica*, B47, 192–197.
- Chopin, C., Ferraris, G., Prencipe, M., Brunet, F., and Medenbach, O. (2001) Raadeite, $Mg_3(PO_4)_2(OH)_8$: A new dense-packed phosphate from Modum (Norway). *European Journal of Mineralogy*, 13, 319–327.
- Kolitsch, U. (1999) Evidence for the identity of meurigite and phosphofibrite by transmission electron microscopy and X-ray powder diffraction. *European Journal of Mineralogy*, 11, Beihefte No. 1, 132.
- (2004) The crystal structures of kidwellite and “laubmannite,” two complex fibrous iron phosphates. *Mineralogical Magazine* 68, 147–165.
- Le Bail, A., Stephens, P.W., and Hubert, F. (2003) A crystal structure for the souzalite/gormanite series from synchrotron powder diffraction data. *European Journal of Mineralogy*, 15, 719–723.
- Lindberg, M.L. and Christ, C.L. (1959) Crystal structures of the isostructural minerals lazulite, scorzalite and barbosalite. *Acta Crystallographica*, 12, 695–697.
- Moore, P.B. (1965) A structural classification of Fe–Mn orthophosphate hydrates. *American Mineralogist*, 50, 2052–2062.
- (1970) Crystal chemistry of the basic iron phosphates. *American Mineralogist*, 55, 135–169.
- Moore, P.B. and Araki, T. (1974) Trolleite, $Al_4(OH)_3(PO_4)_3$: A very dense structure with octahedral face-sharing dimers. *American Mineralogist*, 59, 974–984.
- Moore, P.B. and Kampf, A.R. (1992) Beraunite: refinement, comparative crystal chemistry, and selected bond valences. *Zeitschrift für Kristallographie*, 201, 263–281.
- Redhammer, G.J., Tippelt, G., Roth, G., Lottermoser, W., and Amthauer, G. (2000) Structure and Mossbauer spectroscopy of barbosalite $Fe^{2+}Fe^{3+}_2(PO_4)_2(OH)_2$ between 80 K and 300 K. *Physics and Chemistry of Minerals* 27, 419–429.
- Rømming, C. and Raade, G. (1989) The crystal structure of natural and synthetic holtedahlite. *Mineralogy and Petrology*, 40, 91–100.
- Sejkora, J., Černý, P., Čejka, J., Frýda, J., and Ondruš, P. (2000) K-poor meurigite from the Kněžská hora quarry near Těškov, western Bohemia, Czech Republic. *Neues Jahrbuch für Mineralogie Monatshefte*, 2000, 264–278.
- Selway, J.B., Cooper, M.A., and Hawthorne, F.C. (1997) Refinement of the crystal structure of burangaite. *Canadian Mineralogist*, 35, 1515–1522.
- Sheldrick, G.M. (1997) SHELXL97. Program for the solution and refinement of crystal structures. University of Göttingen, Germany.
- Vencato, I., Mattievich, E., and Mascarenhas, Y.P. (1989) Crystal structure of synthetic lipscombite: a redetermination. *American Mineralogist*, 74, 456–460.
- Walenta, K. and Dunn, P.J. (1984) Phosphofibrit, ein neues Eisenphosphat aus der Grube Clara im mittleren Schwarzwald (BRD). *Chemie der Erde*, 43, 11–16.
- Walenta, K. and Theye, T. (2001) Meurigite von der Grube Clara. *Aufschluss*, 52, 243–246.
- Yakovovich, O.V., Steele I.M., Rusakov, V.S., and Urusov, V.S. (2006) Hole defects in the crystal structure of synthetic lipscombite $(Fe_{4.7}^{2+}Fe_{2.3}^{3+})[PO_4]_4O_{2.7}(OH)_{1.3}$ and genetic crystal chemistry of minerals of the lipscombite–barbosalite series. *Crystallography Reports*, 51, 401–411.

MANUSCRIPT RECEIVED OCTOBER 25, 2006

MANUSCRIPT ACCEPTED MARCH 26, 2007

MANUSCRIPT HANDLED BY SERGEY KRIVOVICHEV